Energy and Technology Review

Lawrence Livermore Laboratory

September 1977

ASER GLASS

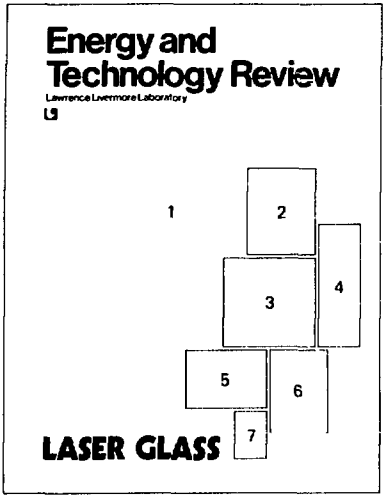

THE COVER

This photographic montage represents some of the research being done at LLL to find laser glasses with optical properties ideal for high-power fusion lasers. These laser fusion systems require large optical elements (amplifier rods and disks, lenses, windows, and Faraday rotators) of high quality.

(1) A 20-cm aperture lens used at the output of Shiva. These glasses must be immune to damage from intense laser beams and must have a low nonlinear index of refraction to avoid self-focusing beam instabilities. The glasses used for amplification must also have high gain coefficients. (2, 3, 4, and 7) Neodymium-doped amplifier disks and rods and Faraday rotator glass. (5) A glass rod being inspected for imperfections. Note the tiny white dots, which indicate minute flaws in the glass. (6) The interior of an amplifier module with a beam diameter of 20 cm. The far end of the module is shown through several elliptical amplifier disks, each set at Brewster's angle to minimize reflection at the surface. Flashlamps, the long glass tubes surrounding the amplifier disks, optically pump these disks.

ABOUT THE JOURNAL

The Lawrence Livermore Laboratory is operated by the University of California for the United States Energy Research and Development Administration. The Laboratory is one of two nuclear weapons design laboratories in the United States. Today nearly half of our effort is devoted to programs in magnetic and laser fusion energy, biomedical and environmental research, applied energy technology, and other research activities.

The *Energy and Technology Review* is published monthly to report on accomplishments in this energy and environmental research and on unclassified portions of the weapons program. A companion journal, the *Research Monthly*, reports on weapons research and other classified programs. Selected titles from past issues of the *Energy and Technology Review* are listed opposite the inside back cover.

UCRL-52000-77-9
Distribution Category UC-2

September 1977

Energy and Technology Review

Lawrence Livermore Laboratory

Prepared for ERDA under contract No. W-7405-Eng-48

MECHANICAL STRAIN EFFECTS IN LARGE MULTIFILAMENT SUPERCONDUCTORS

For over three years we have been conducting a program to develop multifilament niobium-tin (Nb_3Sn) superconductors suitable for use in magnetic fusion confinement magnets. Although the mirror fusion test facility, now being constructed, will use a niobium titanium (Nb-Ti) conductor, future experiments could benefit significantly from the higher magnetic fields that are possible with Nb_3Sn.

In the past, large Nb_3Sn superconducting magnets could not be reliably designed because no one knew exactly how the conductors would behave under mechanical strain. The electrical performance of Nb_3Sn is sensitive to the mechanical forces applied during operation in a magnet. The critical current I_c (the current above which Nb_3Sn is no longer a superconductor for specific values of the magnetic field and temperature) is a rapidly varying function of mechnical strain because Nb_3Sn is very brittle.

To quantify this effect and to learn how to make magnets of these conductors, we have constructed a large cryogenic tensile-test apparatus. Its design permits two measurements: mechanical properties at temperatures of 300, 77, and 4.2 K, and critical current values under simulated operating conditions at 4.2 K as a function of strain and magnetic field. The maximum operating parameters of the machine include loads of 223 kN, magnetic fields of 12 T, and conductor currents of 10 kA.

During the past year we tested a number of large prototype conductors containing up to about 259 000 Nb_3Sn filaments about 5 μm in diameter. Figure 1, based on data collected from these tests, shows how I_c varies with elongation. At first the critical current increases, apparently because the tension relieves compressive strains remaining in the material from the heat treatments it underwent during fabrication. (For a discussion of the fabrication process, see the December 1975 *Energy and Technology Review*—UCRL-52000-75-12, p. 8.) At about 0.3% elongation the internal and external strains become equal, leaving the conductor in an unstrained state and the critical current at maximum.

These tests show that the critical current in Nb_3Sn remains at or above its initial value up to strains of 0.6%. This fact implies that we can design

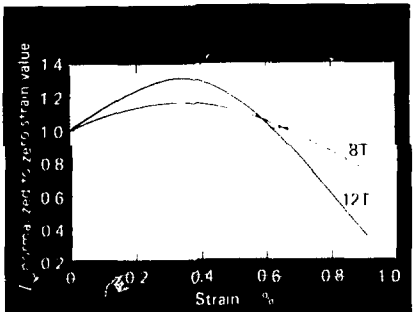

Fig. 1. Variation of current-carrying capacity (critical current I_c) with strain (elongation) for prototype niobium-tin (Nb_3Sn) superconductors carrying currents of 1 to 4 kA in magnetic fields of 8 to 12 T. The initial increase in I_c is attributable to the relief of internal compressive strains by the applied stress.

and build Nb_3Sn magnets with conventional structural strain levels, as we do with Nb-Ti. Furthermore, large Nb_3Sn conductors stretched as much as 0.8% can still recover upon reduction of the load. This property provides an important margin of safety from irreversible damage.

We now have enough data to begin designing prototype test magnets of Nb_3Sn. Successful completion of magnet testing, several years hence, would enable us to design larger fusion containment magnets operating at fields up to 12 T.

Contact Daniel W. Deis (422-6715) for further information on this subject.

ADVANCED ENERGY SYSTEMS

Neutral Beams for Magnetic Fusion

Significant advances in forming energetic beams of neutral hydrogen and deuterium atoms have led to a breakthrough in magnetic fusion: neutral beams are now heating plasmas to thermonuclear temperatures, here at LLL and at other laboratories. For example, in our 2XIIB experiment we have injected a 500-A-equivalent current of neutral deuterium atoms at an average energy of 18 keV, producing a dense plasma (10^{14} particles/cm^3) at thermonuclear energy (14 keV or 160 million kelvins). Currently, LLL and LBL are developing beam energies in the 80- to 120-keV range for our upcoming MFTF experiment, for the TFTR tokamak experiment at Princeton, and for the Doublet III tokamak experiment at General Atomic. These results increase our long-range prospects of producing high-intensity beams of energies in the hundreds or even thousands of kilo-electron-volts, providing us with optimistic extrapolations for realizing power-producing fusion reactors.

The Laboratory's principal task in the national program for magnetic fusion is to develop the magnetic mirror approach—one of several ways to confine the plasma that undergoes fusion and one we have pioneered since the early 1950's. Much progress has been made in recent years to solve the problem of confining the plasma; the major problem of generating and heating the plasma is being solved with neutral beams. Beams of neutral particles (atoms) have been very successful in supplying and replacing particles and energy. Because they have no charge, they cross magnetic fields. They are then ionized by collisions within the plasma and become trapped in the magnetic field. Neutral beams can also heat toroidal confinement machines, but the particle energy required for penetration into the plasma is too high for supplying fuel ions to these plasmas.

We first used neutral beams at the kilowatt level in the Alice experiment (which later became Baseball). Several years later, however, extrapolation of the requirements for our 2X experiment showed that a megawatt level would be needed to reach our experimental goals. As a result, the Lawrence Laboratories (Livermore and Berkeley) launched an effort to develop new beam systems. This effort led first to beam modules that gave 10-A-equivalent amounts at 15 keV (average), then to 50-A-equivalent currents and energies of 20 to 40 keV used in the 2XII experiment.[1] The tandem

Contact Buck Hooper 422-6793 for further information on this article.

mirror experiment (TMX),[2] under construction, will use beams similar to those of 2XII; the mirror fusion test facility (MFTF),[3] also under construction will use 80-keV beams. More recent developments[4] have produced beams with peak energies of 120 keV. Long-range goals include intense beams at energies of hundreds and even thousands of kilo-electron-volts. This work and parallel efforts at the Oak Ridge National Laboratory and elsewhere in the world have resulted in a breakthrough in our ability to generate plasmas at thermonuclear temperatures.

In this article we describe the physics of neutral beams, the state of beam development, and our joint (LLL and LBL) research to produce beams of very high energy at high efficiency. LBL has had principal responsibility for the design, construction, and testing of the positive ion source. LLL assisted in this effort in engineering certain subassemblies—the extraction grids, for example—and in some phases of the fabrication. The 2XIIB facility at LLL was, of course, the full-scale application of these developments. LLL has taken the lead in developing negative ion sources. The high-voltage

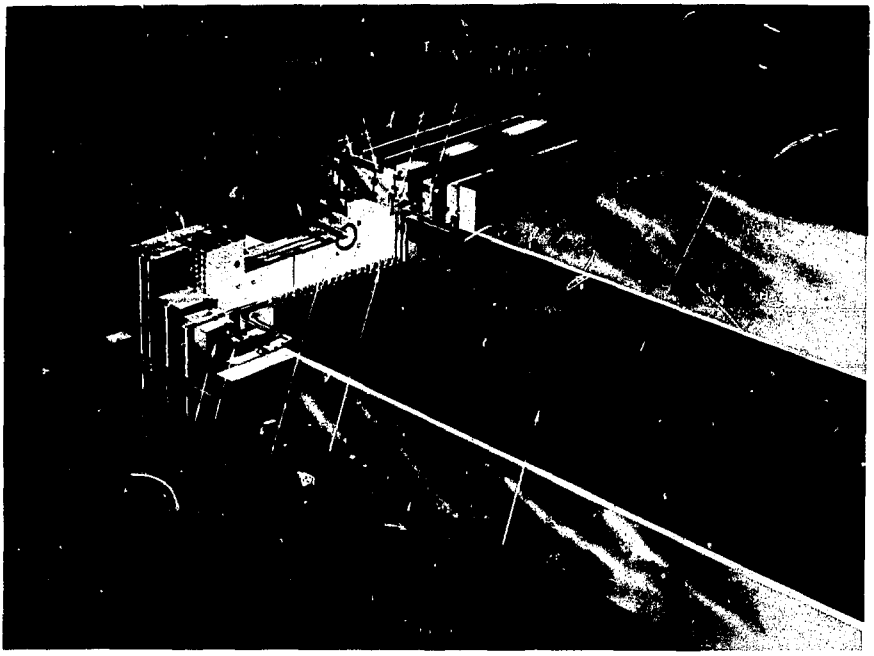

Fig. 1. Cutaway of neutral beam module. This source produces a 50-A-equivalent current of neutral deuterium atoms at an average energy of 18 keV. The current drawn between the filaments and the anode ionizes the deuterium gas to about 1%, roughly 10^{12} ions/cm^3. Positive ions and neutrals stream through defining accel-decel grids. Subsequent charge-exchange collisions between the positive ions and the deuterium gas result in a beam of neutral deuterium atoms having almost the full energy of the extracted positive deuterium ions. The plasma chamber is virtually free of magnetic fields, and the source plasma in the chamber is free of instabilities and turbulence. The uniformity of this source plasma is one of the factors contributing to achieving the small angular divergence of the emitted beam. Twelve of these modules are used in the 2XIIB; 24 will be used in MFTF.

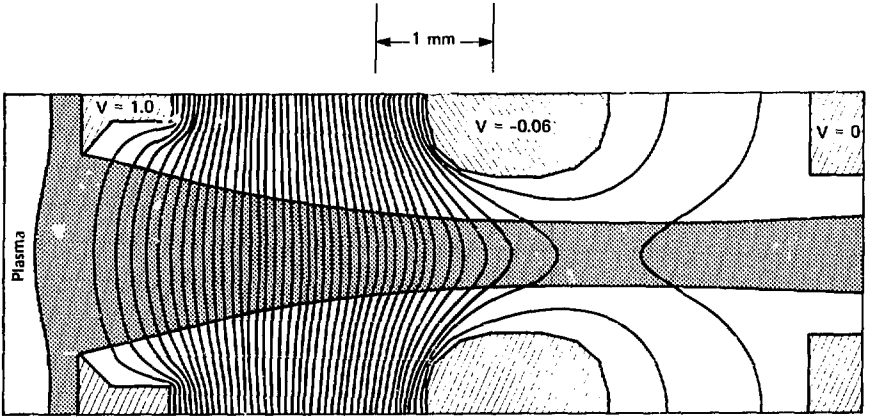

Fig. 2. Electric field potentials and envelope of ion trajectories in the accelerating grids of the source illustrated in Fig. 1. Voltages are normalized to 20 keV. The extraction potential is, thus, 20 keV. The beam neutralization chamber is to the left. The careful computer optimization of the spacing and shaping of these grids was essential in achieving the small (about 1°) angular divergence of the emitted beam.

test stand is being constructed at LLL for developing neutral beam sources based on both positive and negative ions.

NEUTRAL BEAM FORMATION

The first step in forming a neutral beam is to produce deuterium ions for subsequent acceleration by electric fields and eventual conversion to neutrals. This first step occurs in a plasma chamber or "arc box," such as the one shown in the neutral beam module illustrated in Fig. 1. An intense electrical discharge (typically 3500 A), created by current drawn from hot tungsten filaments, ionizes about 1% of the deuterium gas—at 1.3 mPa pressure (10 μTorr)—to form a plasma. The gas is injected through a gas inlet. Interactions in the plasma and on the chamber walls produce an ion mixture of 75% D^+ and 25% D_2^+ and D_3^+.

Ions from the plasma continually bombard the chamber walls. Some pass through slots of a grid mounted on the front wall and are accelerated by voltages applied between this and additional grids. A fraction of the ions is then converted into neutral atoms through charge-exchanging collisions with the deuterium gas in the neutralized section. The resultant beam includes atoms at energies of the full accelerating potential (from D^+ ions) as well as at one-half and one-third energies (from the D_2^+ and D_3^+ ions. [5] The fraction of ions converted to neutral atoms is high at low ion energies (90% for deuterium at 20 keV), but at high energies (above 50 keV) it drops. Thus, at very high energies, a different technique will be required (discussed later).

BEAM CRITERIA

A neutral beam must satisfy several criteria to be effective. One is that beam power injected into the magnetically confined thermonuclear plasma must be as high as possible. Consequently, beam "optics" are critical. To a large extent, the optics are determined by the electric fields in the accelerating grids. The space charge in the extracted ion beam is high, necessitating computer analysis of the particle trajectories within the accelerator grids. Figure 2 shows a computer plot of the electric potentials and the envelope of ion trajectories within the grids of Fig. 1. The electrons in the arc box plasma are repelled by the applied electric potentials, which are

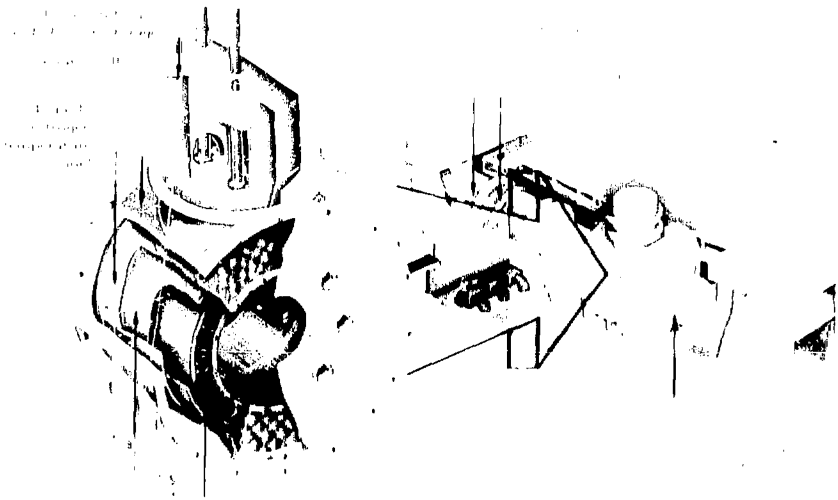

[illegible] high electric potential; hence, the need for the insulating support.

[illegible]

TEST FACILITIES

[illegible]

operate for long pulses (30 s and more) at energies as high as 200 keV. The output voltage can be either positive or negative, allowing it to be used in negative ion development, which we discuss later.

Deuterium beams striking a target saturated with deuterium are predicted to produce as many as 10^{12} neutrons/s, posing a serious radiation hazard. As a result, the HVTS beam line is located inside a concrete-shielded room. The radiation level at the outside of the concrete walls will be less than the maximum permitted dose for personnel, even during the most intense beam operations. In contrast, our other test stands are not shielded and must use hydrogen instead of deuterium for high-voltage, long-pulse operation.

In the HVTS, the deuterium gas accompanying the neutral beam is vacuum-pumped at 500 kl/s by a cryocondensation pump (Fig. 4). The gas freezes on panels cooled by liquid helium (at 4.2 K). The helium, liquefied in an adjacent room, is confined to a closed-loop system to prevent losses to the atmosphere. Heat loading on the helium, especially by thermal radiation from room-temperature surfaces, is reduced by panels cooled to liquid-nitrogen temperature (77 K), as shown in Fig. 4. Also, the chevrons between the beam and the helium-cooled panels are cooled to 77 K to minimize heat loads.

Our test experience is being used to construct and test beam lines for magnetic fusion experiments. For example, a joint LBL/LLL engineering team is developing the beam line for use in the Princeton TFTR (toroidal fusion test reactor) tokamak. Also, LBL is developing the beam line for the Doublet III tokamak at General Atomic in San Diego. Both

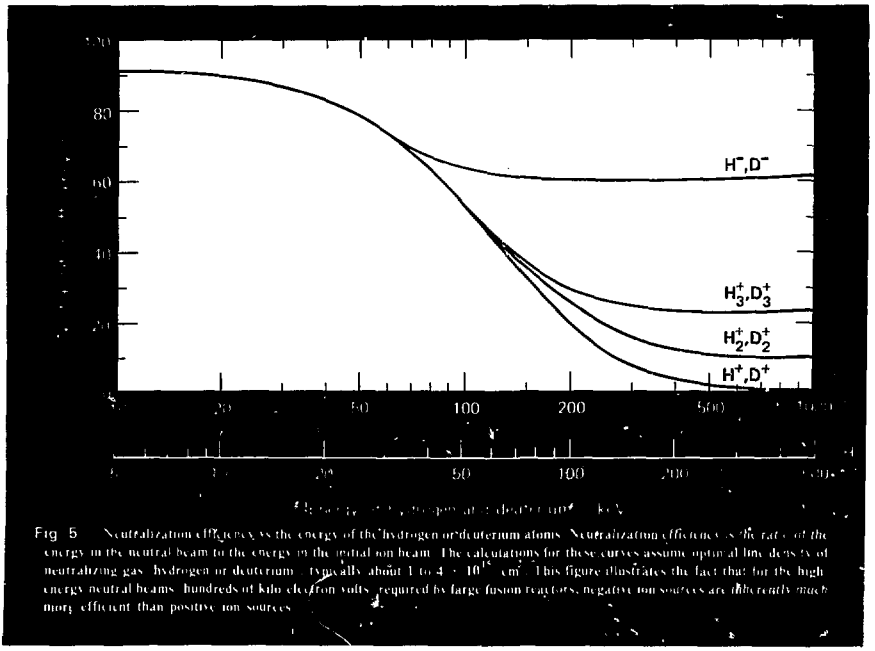

Fig. 5. Neutralization efficiency vs the energy of the hydrogen or deuterium atoms. Neutralization efficiency is the ratio of the energy in the neutral beam to the energy in the initial ion beam. The calculations for these curves assume optimal line density of neutralizing gas (hydrogen or deuterium—typically about $1 \text{ to } 4 \times 10^{15}$ cm^{-2}). This figure illustrates the fact that for the high energy neutral beams (hundreds of kiloelectron volts) required by large fusion reactors, negative ion sources are inherently much more efficient than positive ion sources.

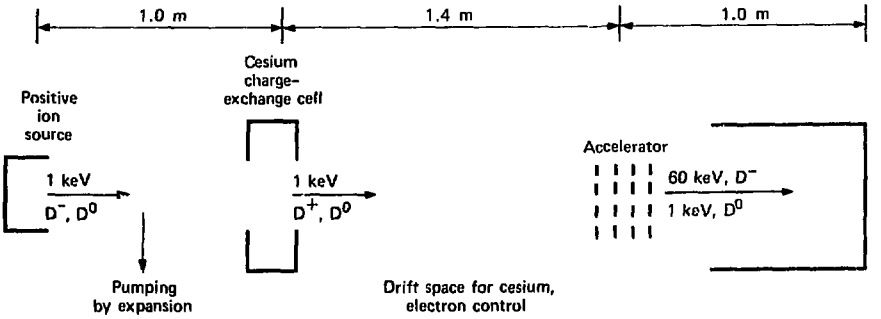

Fig. 6. Schematic of double charge-exchange experiment for producing high-energy D^- beams. The positive ion beam undergoes double charge exchange in the cesium vapor cell at relatively low energy—1 keV. The negative ion beam is then accelerated to the full energy of 60 keV. This experiment has attained D^- currents of 100 mA at 60 keV.

these lines incorporate many features of the HVTS neutral beam. Within LLL, the beam development group also interacts with the mirror confinement group to provide the best neutral beams for the experiments.

FUTURE DEVELOPMENT

Neutral beams for thermonuclear reactors using magnetic fields are predicted to require energies in the range of 200 keV to 1.2 MeV. As mentioned earlier, charge-exchange efficiencies are small at high ion energies, so that most of the accelerated power remains in the ion part of the beam. This limitation will be overcome by using the high efficiency with which an electron can be stripped from a negative ion.[6] As illustrated in Fig. 5, the neutralization efficiency at high energies is at least three times more efficient for stripping negatively charged hydrogen or deuterium ions than for charge exchange on positive ions. We are therefore working on the advanced development of neutral beams based on negative ions instead of positive ions—neutralizing the ion by stripping rather than by charge exchange.

The neutralization efficiency for negative ions can be made larger than that indicated in Fig. 5 by stripping the beam in a highly ionized plasma. Efficiencies greater than 80% can be attained. Ultimately, efficiencies close to 100% may be reached with stripping by light: if the energy of the photons is greater than the 0.75-eV binding energy of the extra electron on the deuterium ion, photon–ion collisions can remove the electron. Such stripping will require high-efficiency lasers and a high-quality optical cavity to keep the power required to produce the laser beam acceptably low.

The most difficult part of this development is to produce high-energy negative deuterium ions. Several production techniques are being studied at LLL and elsewhere. The technique we are studying the most intensely is charge exchange in cesium vapor:

$$D + Cs \rightarrow D^- + Cs^+.$$

The efficiency of this process is 24% at 1 keV and even greater at lower ion energies.

In this technique[7] a D^+ beam produced, for example, at 1 keV passes through cesium vapor (Fig. 6). Resultant collisions rapidly convert the beam to D^0. Further collisions with the cesium convert 20% or more of the D^0 to D^-; thus, the process is often called double charge exchange. The beam then travels through a drift space, where the density of the deuterium gas accompanying the beam is

reduced to a relatively low level. This space is also used to control electrons, since any electrons in the beam are also accelerated, thereby reducing the production efficiency of the final, high-energy beam. In the drift space, the random kinetic energy of any electrons carries them away from the beam, leaving a beam whose space charge is neutralized by background positive ions. At the time of writing, a current of about 100 mA of negative deuterium ions had been accelerated to 60 keV. We plan to develop a larger system that will provide 1 MW of D^0 at 200 keV—a major step in the development of high-energy neutral beams for experiments and reactors.

Key Words: high-energy neutral beams; ion beams; magnetic fusion; magnetic mirrors; neutral beams.

NOTES AND REFERENCES

1. For an overview of the LLL magnetic fusion energy program and a description of the 2XII experiment, see the June 1976 *Energy and Technology Review* (UCRL-52000-76-6), p. 1.
2. The TMX experiment is described in the July 1977 *Energy and Technology Review* (UCRL-52000-77-7), p. 1.
3. For a description of the MFTF experiment, see *A Mirror on Energy*, Lawrence Livermore Laboratory, Brochure B-090 (May 1977).
4. For further information, see K. W. Ehlens, K. H. Berkner, W. S. Cooper, J. M. Haughian, W. B. Kunkel, B. A. Prichard, Jr., R. V. Pyle, and J. W. Stearns in *Proceedings 9th Symposium on Fusion Technology, Garmisch, W. Germany, June 1976*; also available as Lawrence Berkeley Laboratory, Rept. LBL-4471 (1976).
5. For details on neutralization efficiencies, see K. H. Berkner, R. V. Pyle, and J. W. Stearns, *Nuclear Fusion* **15**, 249 (1975).
6. A general discussion of high-efficiency beams was presented by E. B. Hooper, Jr., at the *International School of Plasma Physics: Third Symposium on Plasma Heating in Toroidal Devices, Varenna, Italy, September 1976*; also available as Lawrence Livermore Laboratory, Rept. UCRL-78623 (1976).
7. The current status of this experiment was reported by E. B. Hooper, Jr., O. A. Anderson, T. J. Orzechowski, and P. Poulsen at the *Symposium on Negative Ion Beams, Brookhaven National Laboratory, Upton, New York, September 1977*; also available as Lawrence Livermore Laboratory, Rept. UCRL-80102 (1977).

ENVIRONMENT AND SAFETY

Microwave Gas Analyzer Development at LLL

Air-pollution control efforts have long been hampered by the need for adequate instrumentation. Since the mid-1960's, LLL has worked to fill this need, developing an increasingly more sophisticated series of monitors, detectors, and gas analyzers based on microwave spectroscopy. One of our instruments has achieved unprecedented sensitivity, detecting (on a cycle of four data points per hour) less than 1 ppb of ammonia in air. Another continuously measures ammonia in the range 200 to 1000 ppb in our Imperial Valley environmental survey. A recent development is a monitor that is specifically sensitive only to water vapor. Another instrument, considerably less specialized, will measure any of 10 common hazardous solvents in concentrations as low as one-fifth of safe occupational limits. Future developments now in the planning stage include an inexpensive process-control monitor to continuously analyze the products of a chemical reaction and a hand-held personal monitor to check for local hazards such as carbon monoxide.

Contact Lawrence W. Hrubesh (422-6385) for further information on this article.

Inadequate instrumentation is a difficulty that has plagued air-pollution control efforts since their inception. Existing methods for measuring many of the irritants and poisons in the air have been cumbersome and unautomated, relying on bulky equipment and time-consuming procedures. Samples are collected in the field, carried to a laboratory, and analyzed by chemical methods. By the time analysis is completed, much environmental damage may already have taken place.

To overcome this difficulty, LLL has developed a series of instruments based on microwave rotational spectroscopy. These instruments can cope with the detection and analysis problems associated with a wide variety of pollutants and the extremely small, yet significant, concentrations in which these pollutants may occur.

The potential of microwave rotational spectroscopy for chemical analysis was recognized early. This potential, however, was not realized until the late 1960's when commercial instruments became available. In the mid-1960's we set out to produce microwave instrumentation with optimum sensitivity that could search for spectral information

from transient species within a complex gas mixture during fast chemical reactions. We developed a very sensitive search spectrometer having a resonant cavity as the absorption cell [1] and used it to detect transients such as OH and NF_2 in reactive mixtures. [2]

A major technological advance in microwave generation occurred when Gunn-effect diodes came on the market. Gunn diodes are small, low-power, solid-state microwave generators whose output frequency is easily tuned and stabilized. They quickly replaced large high-voltage vacuum tubes as reliable excitation sources for microwave rotational spectroscopy.

Soon after the Gunn diodes became available we demonstrated a simple, sensitive, and compact spectrometer [3] which combined the diode with a small resonant cavity (Fig. 1). Various agencies concerned with environmental monitoring, recognizing the possibility of incorporating such a device into a portable gas analyzer, commissioned us to develop prototype instruments for specific gases. The microwave technique was particularly exciting because it offered the high resolution needed to determine unambiguously the kinds and amounts of pollutants in the atmosphere.

Fig. 1. The absorption cell of a typical microwave rotational spectrometer. The upper portion between the two flanges is the resonant cavity surrounded by a heater (black band); the lower portion is a housing for some of the associated electronics. The heater varies the length of the cavity by thermal expansion, thereby controlling its resonant frequency. In one of the rectangular blocks on the top flange there is a tiny Gunn diode for producing the microwaves. The other block houses a different kind of diode for detecting them. The two stainless-steel fittings are vacuum connections, one to the vacuum pump and one to the device for admitting the gas sample.

OPERATION

A microwave spectrometer consists basically of three main components: a microwave radiation source, an absorption cell in which to expose the gas to microwave radiation, and a microwave detector (Fig. 2). The source radiates microwaves at a constant power level, and the detector records the amount of microwaves not absorbed by the gas. The absorption is strongly dependent on frequency; tuning the source through a frequency range produces a series of sharp, well-separated dips in the detector output, a microwave absorption spectrum that is uniquely characteristic of the gas in the absorption cell. Figure 3 is part of the microwave absorption spectrum for methanol.

The widths of the absorption dips depend on the gas pressure in the absorption cell; at ordinary pressures the dips become so broad and shallow as to be undetectable. Practical spectrometers, therefore, operate at pressures of 30 Pa (230 μm Hg) or less. In our system a vacuum pump maintains the low pressure, and the injection cell supplies the analysis gas at a rate compatible with the pump's speed.

This system employs a modulated input signal and a narrow-band, phase-sensitive (lock-in-

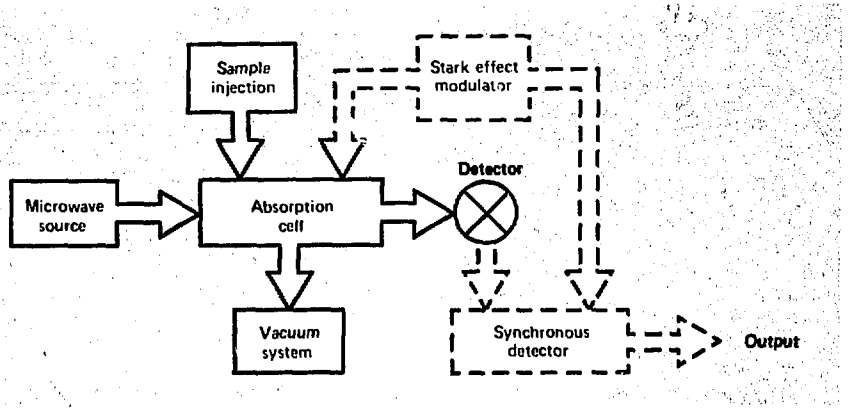

Fig. 2. Simplified block diagram of a typical microwave spectrometer. The main components are the microwave source, the absorption cell, and the detector. The vacuum system is an important auxiliary; the microwave absorption lines become sharp only at pressures below about 30 Pa. The Stark effect modulator and the synchronous detector are auxiliaries that greatly improve the signal-to-noise ratio.

amplifier) detector to improve the signal-to-noise contrast. A passive detector whose output depends only on the incoming signal gives a constant signal for a constant input. Direct-current signals are hard to amplify; random fluctuations, which occur on any signal and are easy to amplify, grow out of proportion and obscure the absorption lines. To circumvent this difficulty, the incoming signal is chopped into a series of pulses, typically at over 5 kHz. The detector amplifier is specially tuned to this modulation frequency. The random fluctuations are small in comparison to the difference between signal on and signal off, and the result is a greatly improved signal-to-noise ratio.

Signal chopping is accomplished by applying a pulsed electric field across the gas in the absorption cell, where the Stark effect changes the absorption spectrum of the gas, splitting each sharp spectral line into a number of weak ones that appear only when the electric field is on. Between pulses the absorption spectrum remains normal. Above the baseline the detector displays absorption lines that are in phase with the pulsed electric field; below the baseline are displayed only those lines that appear when the electric field is off (the normal spectrum). Figure 3 was produced in this way and shows both kinds of lines.

Gunn diodes and other microwave oscillators generate highly monochromatic radiation in the frequency range 3 to 300 GHz, corresponding to wavelengths of 100 to 1 mm. Optical spectroscopy deals with infrared, visible, or ultraviolet light; prisms, gratings, mirrors, and slits are used for analyzing the wavelengths present and observing absorption lines. Microwave radiation, on the other hand, is transmitted through circular or rectangular waveguides and analyzed by electronic techniques. In some spectrometers the waveguide doubles as the absorption cell.

In a waveguide absorption cell the microwave radiation passes through the gas only once; the waveguide must therefore be long to give measurable absorption. For compactness our spectrometer uses a resonant cavity for the absorption cell. Here, the microwave radiation reflects back and forth many times, multiplying the amount of radiation absorbed.

As in ultraviolet, visible, or infrared spec-

Fig. 3. Partial microwave absorption spectrum (signal vs frequency) for methanol, showing the sharp resonances (downward dips) characteristic of pure rotational spectra. The peaks above the baseline are artifacts of the Stark effect; the signal is processed to display them above the line to prevent their being confused with the normal spectrum lines. This small and easily ignored distortion of the baseline is a small price to pay for the vast improvement in the signal-to-noise ratio resulting from signal modulation by the Stark effect.

troscopy, the microwave absorption spectrum arises from transitions between energy levels. The frequency at which the absorption takes place corresponds to the energy difference between two states. The mechanisms that cause the four spectra, however, differ. Ultraviolet and visible spectra arise from transitions between electronic energy levels, infrared spectra arise from transitions between molecular vibrational energy levels, and microwave spectra arise from transitions between molecular rotational energy levels.

The rotational motion of molecules in the gas phase is quantized into discrete states with sharply defined energy values. The energy difference between rotational states is slight compared to the vibrational energy. Thus, many rotational states are populated at normal temperatures. Because the spectral lines can be made very narrow at low enough pressures (typically having a full width at half maximum of 0.000 02 wavenumbers at pressures of 30 Pa) and because the microwave radiation is coherent, monochromatic, and tunable, no other present form of molecular spectroscopy has a higher resolution than microwave rotational spectroscopy.

DEVELOPMENT AT LLL

In 1973 existing wet-chemical analytical methods showed that formaldehyde is a major constituent of automobile exhausts and also that it is virtually absent in the air, even in cities. Evidently the formaldehyde is destroyed soon after it leaves the tailpipe, but the 1973 methods were unable to trace the course or identify the products of the reactions. For this reason the Environmental Protection Agency was seeking an analytical instrument not only sensitive enough to detect very small quantities of gases but also simple to use, reliable, and portable. Microwave spectroscopy was attractive because it is selective; its output is unaffected by interfering gases.[4] Also, combining miniature solid-state diodes with small but highly effective resonant cavities made simple, portable instrumentation feasible.

The prototype instrument,[5] which we completed and delivered to the Environmental Protection Agency in 1974, was only partly successful. Although its selectivity and accuracy were much better than those of the wet-chemistry methods for analyzing exhaust samples, its sensitivity of about 500 ppb was inadequate for ambient air measure-

Fig. 4. Pen recorder trace showing the response of a microwave ammonia monitor to the addition of a trace of ammonia (about 10 ppb) to the air being sampled. In this mode the microwave spectrometer is operated on a fixed frequency corresponding to one of the major absorption lines of ammonia. The signal controlling the recorder pen is made proportional to the deviation of the microwave signal from its full (nonabsorbed) strength.

Fig. 6. *A recorder trace illustrating* how preconcentration increases the sensitivity of ammonia detection. At the start (*left*), the trace shows the detector response to 500 ppb of ammonia without preconcentration. When the flow is diverted to pass through the trap, the response drops essentially to zero. After accumulating for about an hour, the ammonia begins to leak out (breakthrough). Heating the trap releases the accumulated ammonia, causing a large detector response. By this means it is possible to detect ammonia traces as low as 0.8 ppb.

ments. Since formaldehyde in exhaust is currently only of research interest, the market for such a formaldehyde monitor is inadequate to attract a commercial manufacturer.

Our next such instrument, an ammonia-vapor monitor for the California Air Resources Board, was much more satisfactory. We designed a membrane prefilter into the instrument; the prefilter selectively admits ammonia to the vacuum system while holding back most of the other constituents of the sample, boosting the instrument sensitivity to better than 50 ppb of ammonia in ambient air. This is the highest sensitivity ever achieved for continuous detection of any gas by microwave spectroscopy. Figure 4 shows how the output of this monitor responds to the addition of 10 ppb of ammonia to a stream of pure air.

Near the end of our prototype ammonia-monitor development the Environmental Protection Agency, which had been following our work, requested that we try to extend the instrument's sensitivity to 1 ppb or below. This problem was solved by designing a modular attachment that automatically preconcentrates the sample, trapping the ammonia on a special chromatographic material (Chromosorb 104) for 10 minutes and then releasing it to the microwave absorption chamber in a burst.[6] Figure 5 illustrates one operating cycle of this monitor. Although its operation is thus intermittent, the instrument can detect as little as 0.8 ppb of ammonia in a laboratory-prepared sample. It is now being tested by both the California Air Resources Board and the Environmental Protection Agency, and it may be adopted as a standard method for trace ammonia detection in air.

Meanwhile, the ammonia-vapor monitor has

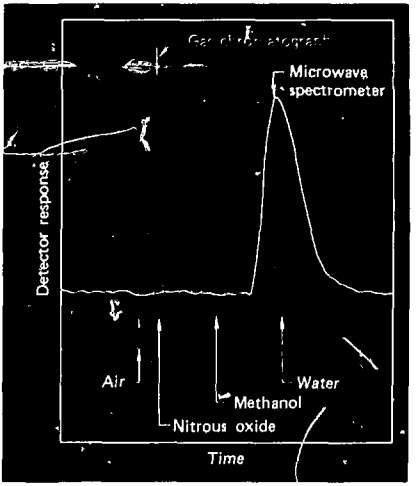

Fig. 6 — Superimposed responses of a gas chromatograph and a microwave spectrometer sampling the same gas flow, showing the selectivity of the microwave spectrometer. The gas chromatograph was injected with a mixture of air, nitrous oxide, methanol, and water vapor. It separated these components and recorded the emergence of each as a separate peak. (Blue trace.) *The microwave spectrometer, white trace, ignored the first three constituents and responded to the water vapor only.*

CURRENT AND FUTURE DEVELOPMENTS

The National Institute of Occupational Safety and Health, responsible for recommending appropriate instrumentation for occupational safety measurements, has asked us to develop a prototype multihazard spectrometer. What is required is a portable instrument capable of unambiguously detecting a number of toxic vapors. Since many toxic vapors absorb microwaves, it appears feasible to base such an instrument on microwave rotational spectroscopy.

The 10 common solvents listed in Table I are

The instrument must be reliable, easy to operate and portable. To meet these requirements we have introduced a new approach. Permeation tubes are designed into the instrument. These tubes emit a *constant flow* of the gases of interest, serving both as references to stabilize the microwave source and as sources for instrument calibration. The readout is simplified to a meter reading, with a selector for switching from one gas to another.

To make the instrument even more portable, we intend to make it smaller than 0.08 m³ and lighter than 18 kg. The instrument development is about half complete, with a crude working model now being tested. A finished instrument is expected in the spring of 1978.

Table 1 Threshold limit values adopted by the National Institute for Occupation.. Safety and Health as a basis for specifying the performance of a multihazard spectrometer and the minimum detection limits derived from them

Compound	Limit, ppm	Minimum detection limit, ppm
Acetaldehyde	100	20
Acetonitrile	40	8
Acrolein	1000	200
Ammonia	25	5
Carbonyl sulfide	60	12
Ethanol	1000	200
Ethylene oxide	50	10
Isopropyl alcohol	400	80
Methanol	200	40
Propylene oxide	100	20

NATIONAL SECURITY

Glasses for High-Power Fusion Lasers

Neodymium-doped glass lasers, such as those in LLL's Shiva laser system, offer the best chance for early demonstration of the scientific feasibility of inertial confinement fusion. The output of these high-power lasers is determined by the media used for their amplifying and transmitting components. Our research has shown that significant increases in performance are possible with new fluoride-base glasses that have low refractive indices. These new glasses form the basis for more powerful experimental solid-state lasers and are potentially useful for advanced fusion laser systems.

A means for the practical conversion of nuclear power to electrical power may be by inertial confinement fusion. We anticipate that the earliest demonstration of the scientific feasibility of this concept will be by means of laser-induced implosion of D–T pellets. In the past few years, considerable progress has been made in the development of powerful laser systems capable of igniting ever-increasing quantities of inertially confined nuclear fuel.[1] The most advanced lasers for this purpose use

Contact Marvin J. Weber (422-5486) for further information on this article.

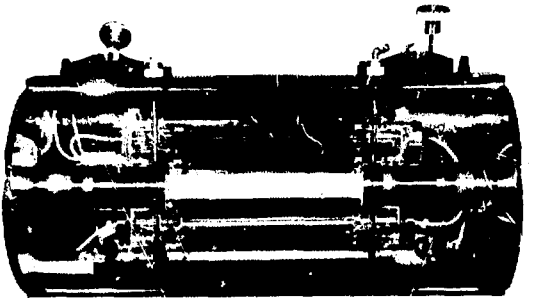

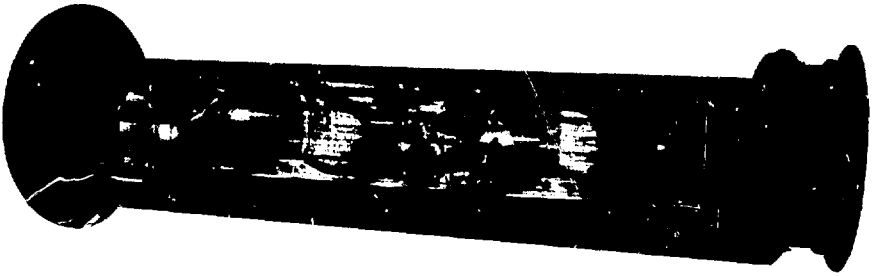

Fig. 1. Fusion laser amplifiers. The amplifying medium is neodymium-doped silicate glass. (*Top*) Rod amplifier. The laser rod is 5 cm in diameter and is surrounded by an array of xenon flashlamps that serve as the optical pump. (*Bottom*) Disk amplifier. The elliptical laser disks are 15 × 30 × 3 cm and are oriented at Brewster's angle to minimize reflections.

neodymium-doped glass as the amplifying medium. Typical rod and disk amplifiers are shown in Fig. 1. These components are arranged in chains of increasing apertures as shown in Fig. 2. The resulting systems are able to concentrate many terawatts of optical power onto targets of less than a millimetre in times of less than a nanosecond.

It became apparent at an early stage in the glass laser development program at LLL that future fusion laser development would be limited by the properties of the laser optics. Lasers based on both Nd-glass amplifier media, as well as gas amplifier media, use glass and crystalline optical materials extensively. The nonlinear propagation properties, the damage levels, and the ease of manufacture of large-aperture optics define the performance of all of these systems. In the case of Nd-glass laser systems, additional attention must be paid to the lasing properties of the glass amplifier media. When we began to study the effect that glass lasing properties and nonlinear propagation properties had on system performance, we found that remarkable increases in laser system performance were available if materials with high gain and low nonlinear refraction index could be found. These properties have now been realized with the fabrication of large pieces of fluoride-base laser glass. These materials have permitted us to extend our solid-state laser designs from the 30-TW Shiva laser to the 200- to 300-TW Nova laser and to conceive of a 1000-TW solid-state reactor-test laser.

Glass is used in several laser components.[2] The primary use is for the amplifying components—presently silicate glass with neodymium dopant. Glass is also used for light-transmitting components (such as lenses, windows, and substrates for thin-film polarizers and beam splitters) and for Faraday rotation in optical isolators. For laser beam diameters up to 50 cm, glass is an attractive medium since it can be made in large sizes with the requisite high optical quality; in fact, a limiting size for glass components has not been reached.

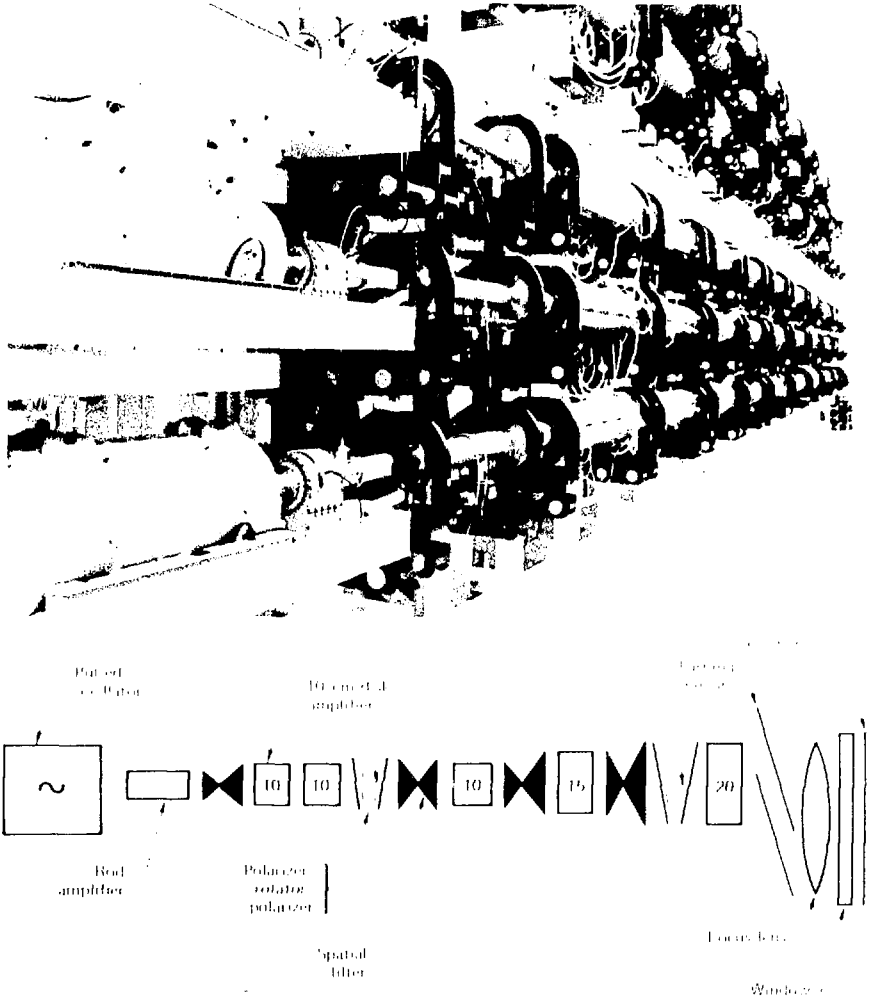

Fig 2 Typical staging sequence of fusion laser components. The actual installation of components in the Shiva laser system is shown in the photograph above. A schematic representation of a single chain is shown in the line drawing below. Each component in the chain must be optimized for the increasing beam-power levels (left to right). Numbers represent the minor axis diameter of the elliptical glass disks in centimetres. The total length of the chain is about 50 m.

The [illegible] reference [illegible] in which they are [illegible] must have [illegible] glass [illegible] low [illegible] birefringence [illegible] workability [illegible] standard [illegible] flatness. It [illegible] matched [illegible] parasitic suppression [illegible] coating. The [illegible] power beams is dependent on its nonlinear optical response, or nonlinear index of refraction. Thus, glasses that have low nonlinear response can sustain very high power densities throughout. Finally, the glass must withstand the intense ultraviolet flux from the flashlamp without darkening or incurring physical damage.

Because the [illegible] properties of glass [illegible] possible [illegible] [illegible] optimize [illegible].

LASER GLASS RESEARCH PROGRAM

Glass [illegible] required for [illegible] components in a laser amplifier chain such as that shown in Fig. [illegible]. Current glass laser [illegible] uses silicate glasses. For each different component function and for increasing power levels, the required glass properties change. These [illegible] properties as well as cost factors demand that we [illegible] optimization studies for both the glass elements and the component staging.

In the solid-state physics effort at LLL, we are methodically exploring an immense *parameter field* to achieve optimum lasing and optical performance from the glass. Commercial glass manufacturers are supplying glass samples formulated, melted, and configured to our specifications. We measure the physical and optical properties of these samples and then use this empirical information in a set of computer codes to model the glass performance under laser operating conditions.

The resulting laser glass research program has [illegible]

REFRACTIVE INDEX

The [illegible] is the most important [illegible] properties affecting the performance of [illegible] high-power laser lasers. The total refractive index is composed of linear [illegible] and [illegible] components; the nonlinear refractive index is dependent on the material's response [illegible]. [illegible] depends [illegible] on the order of [illegible] 10 GW [illegible] the optical path [illegible] pulses [illegible] long enough (about a [illegible]) to cause phase shifts of several wavelengths in the optical wavefront. These phase shifts can [illegible] the [illegible] of the beam intensity, increase the beam divergence, and even cause destructive self-focusing. The existence of large positive nonlinear refractive indices is, therefore, a major problem to be solved for the improvement of laser glass.

Our early experiments revealed that material with a small linear refractive index, n, and a small dispersion (change in n with change in wavelength) also had a small nonlinear index coefficient, n_2. We have obtained further data on the correlation between linear and nonlinear refractive indices by using time-resolved interferometry on a wide variety of glasses. With these empirical results, we can estimate the nonlinear index from measurements of the linear index and the dispersion.

Optical glasses are conveniently grouped using as coordinates the refractive index, n, and the Abbe number, ν, where ν is *the reciprocal of dispersion*. Regions of n_d and ν_d of known optical glasses are shown in Fig. 3. (*The subscript d signifies that the* properties were measured at the wavelength of the

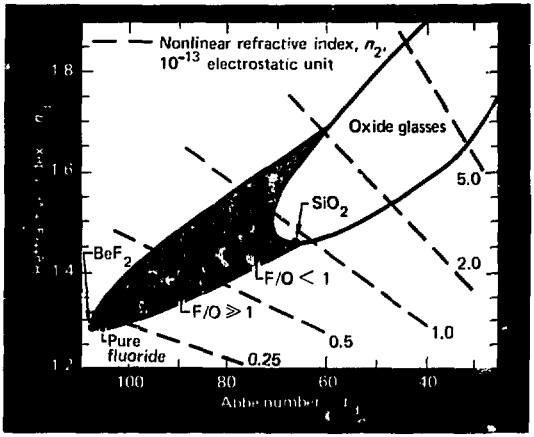

Fig. 3. Optical glasses of varying composition are mapped by their refractive index and Abbe number (reciprocal of dispersion). Superimposed are dashed lines of constant nonlinear index, n_2, based on our measurements. The nonlinear index, n_2, is reduced as the fluorine-to-oxygen ratio (F/O) is increased. The most promising glasses for fusion lasers are those toward the lower left-hand corner.

helium d line—587.6 nm.) Superimposed in Fig. 3 are dashed lines of constant n_2 predicted from the n_d and ν_d values. To propagate laser beams with small distortions, we need low-n_2 glasses; these are the fluoride-containing glasses in the lower left-hand corner of the figure. Various types of fluoride glasses are listed in Table 1.

Table 1. Various types of fluoride-containing glasses. We have investigated those marked with an asterisk for possible fusion laser applications.

Former	Modifier ions
Pure Fluoride Glasses*	
BeF_2	MF (M^+ = Li,Na,K,Rb,Cs)
AlF_3	MF_2 (M^{2+} = Mg,Ca,Sr,Ba,Zn,Cd,Pb)
ZrF_4	MF_3 (M^{3+} = Al, Y, La, Bi)
	MF_4 (M^{4+} = Zr, Th)
Fluoride Glasses Containing Oxygen (F/O[a] > 1)*	
Fluoride glasses containing small mole % phosphate	
Oxide Glasses Containing Fluorine (F/O ≲ 1)	
Fluoroborate	
Fluorosilicate*	
Fluorophosphate*	
Fluorogermanate	

[a] F/O represents the ratio of fluorine to oxygen ions.

The most common commercial optical glasses are oxide glasses, principally silicates and phosphates (i.e., SiO_2- and P_2O_5-base). Current optical glasses with the lowest n_2 values are fluorine-containing oxide glasses, namely, fluorosilicates and fluorophosphates. The glass with the lowest index reported is beryllium fluoride (BeF_2) without any modifiers. BeF_2 forms a glass analogous to SiO_2, but it is more ionic and the BeF_2 bonds are weaker (therefore, it has a lower melting point). Pure BeF_2 and SiO_2 glasses are plotted in Fig. 3 and represent the lowest n_2 values of the fluoride and silicate glass types, respectively. The addition of network modifiers, such as alkali, alkaline earth, aluminum, and other cations, changes the optical properties and yields the n_d–ν_d regions shown.

Because of their small predicted n_2 values, fluoride glasses are the most promising candidates for both passive components (such as lenses, windows, and substrates) and active components (such as the laser-amplifier and Faraday-rotation media). Optical figures of merit two to three times that of present oxide laser glasses may be realized (see

Table 2. Figures of merit for the nonlinear refractive index of optical materials.[a]

Component	Figure-of-merit formula	Silicate glass (ED-2, LSG-91h)[b]	Phosphate glass (EV-2, LHG-7, Q-88)[b]	Fluoro-phosphate glass (LG-810, E-181, LHG-10)[b]	Fluoro-beryllate glass (B-101)[b]
Laser disk (parasitic-limited; at Brewster's angle)	$\frac{n^2}{n_2}$	1.0	1.4	2.3	3.1
Window	$\frac{n}{n_2}$	1.0	1.4	2.3	3.6
Lens	$\frac{n(n-1)}{n_2}$	1.0	1.3	2.0	2.2

[a]A smaller n_2 implies a larger figure of merit and, hence, a better glass. Silicate glasses are currently used in glass lasers at LLL.
[b]Manufacturer's designation.

Table 2). Since fluoride glasses generally have large band gaps, they transmit light over a large spectral range. Hence they are potentially useful as transmitting optical components for high-power lasers operating at various wavelengths with lasing media other than neodymium.

LASING PROPERTIES

In the amplifying element, the important factor is the influence of the host glass on the ability of the lasing ion to absorb light from the optical pumping source, to store this energy, and to release it to amplify the laser beam. Energy storage by the lasing ion is governed by its absorption properties, excited-state lifetimes, and quantum efficiency. The position of absorption bands of rare-earth ions (such as neodymium) in solids shows little change with host, but the relative strength of the bands does change. Thus, the absorption coefficient of the lasing ions is host-dependent.

Lasing ions excited to high-energy electronic states relax nonradiatively (heating the host) to the upper lasing energy level. The lifetime of this metastable state determines how fast the level must be pumped to achieve the excited lasing ion population necessary for lasing.

Also, for each absorbed pumping photon, one lasing photon should come out. The quantum efficiency can be degraded in some hosts if the ion-host interaction causes nonradiative losses. In addition, interactions between lasing ions can also cause self-quenching. This effect limits the useful dopant concentration in the glass; that is, the lasing ion concentration cannot be arbitrarily increased without causing self-defeating losses. Thus, the important parameters of net absorption, rate of excitation, and efficiency are all dependent on the host glass.

The rate of energy yield from a laser amplifier is governed by a product of the optical intensity of the extracting beam and the stimulated emission cross section of the lasing ions. As discussed earlier, the beam intensity is limited by the nonlinear refractive index of the host glass. The stimulated emission cross section is also host-dependent.

The emission cross section of a lasing ion determines the yield of the stored energy and, thus, the amount of its amplification. The best cross section to use depends on the intended operation of the laser. Short-pulse, unsaturated lasers need high-cross-section materials in order to get large gain coefficients with a minimum thickness of glass.

However, if the cross section is too high, parasitic losses (in large amplifiers) and saturation will set in and limit performance. On the other hand, long-pulse, saturated lasers require low cross sections so that large amounts of energy can be stored and extracted without parasitic losses. The cross section must not be too low because excessive flux, capable of causing nonlinear optical distortion, would be required to extract the energy. For any fixed pulse width, there is an optimum cross section. If the cross section is too low, gain is low and too much material (glass) is required in the beam path. If the cross section is too high, saturation and parasitic losses reduce the gain. The optimum cross section generally becomes smaller as the pulse width is increased.

The ideal glass is one for which the emission cross section can be varied by a variation in glass composition without degradation of other desirable properties. However, some interaction is unavoidable; for example, raising the cross section usually increases the fluorescent decay rate. Early studies have shown that in silicate glasses, variations by a factor of three in the cross section were possible by changing the network-modifier ions. Variations in cross section by a factor of five have been observed by varying glass network formers.[4]

An additional consideration is the terminal laser-level decay time. To extract all of the stored energy, the terminal laser state must rapidly relax to the ground state. If the stimulated emission rate is too fast, bottlenecking occurs at the terminal energy level, which reduces the useful energy yield. The relaxation rate of the terminal level is also governed by ion-host interactions and can be varied by selecting different glass compositions.

Different glasses may be optimum for different amplifier stages for reasons other than optimum gain. But the wavelength of peak gain varies with the glass used. In the case of phosphate and fluorophosphate glasses, the wavelength differences of the two glasses are small, and their use can be mixed without a large sacrifice in gain performance. This statement is not true, however, for the combined use of, say, silicate and phosphate glasses or oxide and fluoride glasses. Nor does it apply to passive components.

Table 3 compares the range of spectroscopic properties observed in different glass types of interest. A wide variation in most parameters has been obtained and thus provides the laser designer with a range of material parameters to select in optimizing a laser design.

LASER-GLASS OPTIMIZATION STUDIES

Since the advent of lasers, thousands of glasses have been formulated to investigate the effects of changes in glass network and network-modifier ions on the spectroscopic and lasing parameters of neodymium. This work to a large degree was empirical and was hampered by two difficulties: first, the spectroscopic properties and interactions of rare-earth ions were not completely understood even in a crystal environment; second, the specific uses and applications of lasers were less well defined and, therefore it was not always clear which properties should be optimized. Today, both of these problem areas are better understood, and we have

Table 3. Measured range of variations of neodymium laser glass properties.

Glass type	Nonlinear index, 10^{-13} esu	Peak wavelength, nm	Cross section, 10^{-20} cm^2	Linewidth (FWHM), nm	Fluorescence lifetime, μs
Silicate	≥1.0	1057 to 1062	1.0 to 3.1	28 to 35	300 to 1000
Phosphate	≥0.9	1053 to 1056	2.0 to 4.5	19 to 28	300 to 500
Fluorophosphate	≥0.5	1050 to 1055	2.0 to 4.5	22 to 29	300 to 600
Fluoroberyllate	≥0.3	1046 to 1050	1.6 to 4.0	15 to 24	500 to 1000

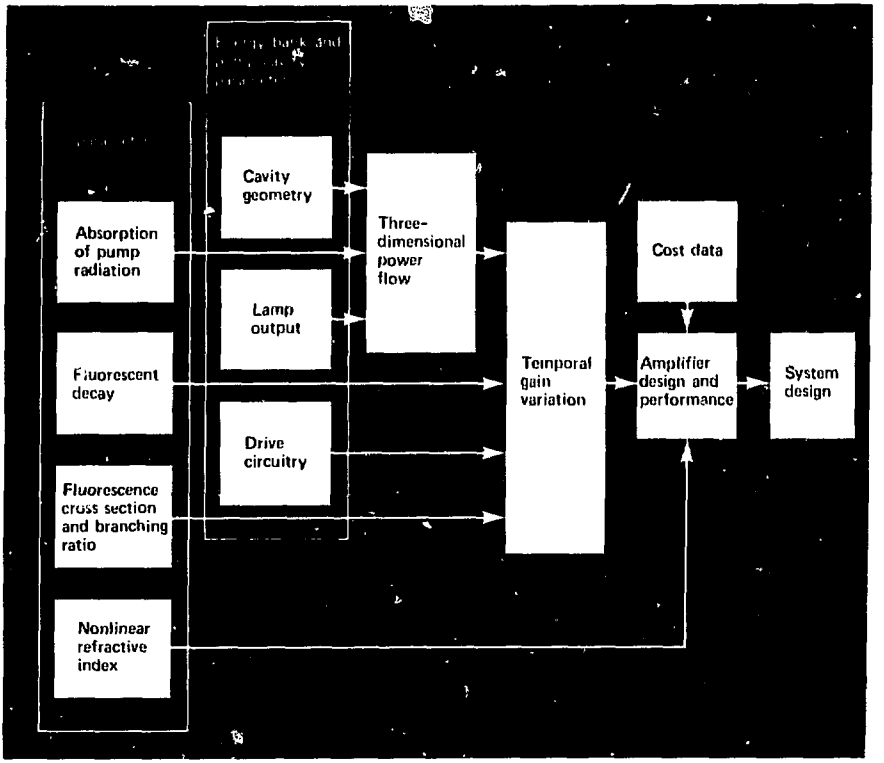

Fig. 4. Schematic flow chart showing laser-system modeling procedure. On the left, the parameters of a specific laser glass are entered into appropriate glass-modeling codes. The next block provides detailed information on the capacitor bank, laser heads, reflectors, flashlamps, and lamp circuitry, which input to the appropriate codes for modeling the power flow and gain variation. The final result of this modeling is the most cost-effective laser system design.

now evaluated over 200 glasses for fusion laser applications.

Predictions of the small-signal laser gain are based on measurements of absorption and fluorescence spectra and decay properties combined with calculations of the effects of flashlamp pumping. We have been successful in using data obtained from small glass melts to:

- Determine lasing parameters from spectroscopic properties.
- Estimate the nonlinear refractive index from linear refractive indices.
- Predict gain of amplifier stages and model the most cost-effective staging of an overall laser system.

From such work, the optimum glasses are selected for the design and staging of individual laser amplifiers in an overall fusion laser system. The lowest-cost system is then chosen for comparison or implementation.

A flow chart for modeling amplifier performance is shown in Fig. 4. The absorption spectrum of the candidate glass is recorded from the near-ultraviolet to the near-infrared. Using the measured line strengths, we derive a set of optical intensity parameters to calculate fluorescence line strengths and to determine the stimulated emission cross section. We also calculate the radiative lifetime and compare it with the observed fluorescence decay rate to determine the quantum efficiency. With data from the per-ion absorption spectrum, a computer program calculates the fractional absorption by the material of the xenon flashlamp radiation. The program contains a model of the flashlamp output spectrum that we modified by rerunning some of the light back through a layer of plasma to approximate the multiple passes that actually occur inside the laser pumping cavity. We then use the output curves of fractional absorption as a function of optical depth in conjunction with decay rate and cross section information to predict the temporal gain of different materials in disk laser amplifiers.[5]

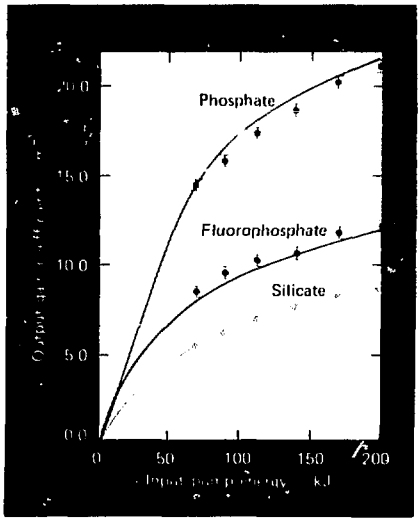

Fig. 5. Comparison of measured (points) and calculated (lines) gain coefficients for three neodymium glasses, using the laser-glass modeling procedure shown in Fig. 4. With all other conditions the same, the mere change to phosphate or fluorophosphate glasses will markedly increase the laser gain or provide the advantage of a much smaller nonlinear index of refraction.

How well does this work? Figure 5 shows the laser amplifier output versus pump energy input for three glasses: a high-gain phosphate, a fluorophosphate, and a low-gain silicate. Shown are a comparison of measured points and predicted gain curves. The overall agreement is within 10% and is typical of the results obtained in our study to date. Because of uncertainties in the accuracy of modeling the pump cavity configuration, data on a silicate glass are normalized to the predictions; however, once this normalization has taken place, there are no other adjustable parameters.

PROGRAM STATUS AND PLANS

Significantly improved neodymium-glass laser performance is now possible with newly developed glasses. We have found that for short-pulse, high-power lasers, the output is nearly inversely proportional to the nonlinear refractive index of the glass, n_2. Glasses with n_2 from one-half to one-third lower than presently used glasses have been identified. The relative figure of merit of these glasses for several laser elements is given in Table 2. In addition, by using phosphate rather than silicate glasses, we have achieved amplifier gain increases greater than 50%.

Commercially available phosphate glasses can have very high gain, but their use in large disk amplifiers is limited because high-gain-induced parasitic losses become dominant. For these large amplifiers, fluorophosphate glasses with medium-high gain and low n_2 are currently the best choice and are the most likely medium for the next larger Nd-glass laser system at LLL (see Fig. 5). The predicted performance of this laser, which we call Nova, is based on the physical parameters of the glasses. Undoped fluorophosphate glasses have been commercially available for some time and are now being formulated and optimized for use in fusion lasers. Beryllium fluoride glass, the ultimate high-power laser medium, is being formulated and tested in small quantities; test results have been very

encouraging, but great uncertainties remain in the production of large, high-optical-quality pieces and in the yields and costs associated with the precautions of handling beryllium.

To ensure that improved glasses will be available in time for Nova, ERDA is supporting developmental research with glass manufacturers in close cooperation with LLL. New glasses are being evaluated in our computer-equipped spectroscopy laboratory[6] where more than a dozen spectroscopic, optical, and physical properties are measured on samples supplied by manufacturers. To hasten development, we provide this information to the manufacturers in the form of data books—to date, in six volumes describing about 200 laser glasses. Large melts of fluorophosphate laser glasses are now being cast into test disks for Nova prototype components.

New ideas in laser design indicate that 10-MJ, 1000-TW solid-state laser systems may be possible. Recent studies also point toward high-average-power systems with efficiencies greater than 1%. These concepts are optimistic, but they may be more reasonable extensions of established glass laser technology than we presently imagine. The accomplishment of laser fusion objectives with advanced lasers based on gaseous laser media will also require imaginative use of optical materials. These lasers are limited by nonlinear, damage, and manufacturing constraints just as solid-state lasers have been. Materials similar to those described in this report will be the basis for the design of future high power lasers.

Key Words glass, glass lasers, neodymium-glass, lasers—materials

NOTES AND REFERENCES

1. The laser fusion program at LLL has been reviewed in two full issues of the *Energy and Technology Review*: February 1976 (UCRL-52000-76-2) and August 1977 (UCRL-52000-77-9). More detailed information on the program is presented in the *Laser Program Annual Report* for 1974, 1975, and 1976, Lawrence Livermore Laboratory, Repts. UCRL-50021-74, UCRL-50021-75, and UCRL-50021-76.
2. M. J. Weber, "Optical Materials for Neodymium Fusion Lasers," in *Optical Materials Problems in Energy Production*, C. Stein, Ed. (Academic Press, New York, NY, 1976), pp. 261-279.
3. E. S. Bliss, D. R. Speck, and W. W. Simmons, "Direct Interferometric Measurements of the Nonlinear Refractive Index Coefficient N_2 in Laser Materials," *Appl. Phys. Lett.* **25**, 728 (1974); D. Milam and M. J. Weber, "Measurement of Nonlinear Refractive-Index Coefficients Using Time-Resolved Interferometry: Application to Optical Materials for High-Power Neodymium Lasers," *J. Appl. Phys.* **47**, 2497 (1976); and "Nonlinear Refractive Index Coefficient for Nd Phosphate Laser Glasses," *IEEE J. Quant. Electron.* **QE-12**, 512 (1976).
4. R. R. Jacobs and M. J. Weber, "Dependence of the $^4F_{3/2}$ - $^4I_{11/2}$ Induced-Emission Cross Section for Nd^{3+} on Glass Composition," *IEEE J. Quant. Electron.* **QE-12**, 102 (1976).
5. For a description of the computer-equipped spectroscopy laboratory, see R. A. Saroyan and M. J. Weber, *Unconventional Spectroscopy*, proceedings of a technical symposium held in San Diego, Calif., August 24-25, 1976 (SPIE, Palos Verdes Estates, Calif., 1976), vol. 82, p. 165.
6. G. J. Linford, R. A. Saroyan, J. B. Trenholme, and M. J. Weber, "Measurements and Modeling of Gain Coefficients for Neodymium Glass Lasers," *Digest of Technical Papers*, 1977 IEEE/OSA Conference on Laser Engineering and Applications, Washington, D.C., June 1-3 (to be published).

PAST TITLES

Articles in the *Energy and Technology Review* have been organized into subject areas approximately corresponding to the Assistant Administrators' areas of responsibility in the Energy Research and Development Administration. These subject areas are listed below with references to some recent articles in each category. (A semiannual index appears in the June and December issues.)

CONSERVATION

Car for Tomorrow: A Quasi-Electric-Drive Vehicle (*June 1977*)
Transportation's Role in the Energy Problem (*March 1977*)
The Methanol Engine: A Transportation Strategy for the Post-Petroleum Era (*December 1976*)

ENVIRONMENT AND SAFETY

Diagnosing Cervical Cancer with Flow Cytometry (*July 1977*)
Phantom Construction: Building a Torso Manikin for Whole-Body Counting (*December 1976*)
Getting the Facts About Ozone (*November 1976*)

FOSSIL ENERGY

Progress in Oil-Shale Research (*February 1977*)
Hoe Creek No. 1: An *In Situ* Coal Gasification Experiment (*January 1977*)

LABORATORY TRENDS

Continuing Education at LLL (*May 1977*)
The Laboratory: Retrospect and Prospect (*February 1977*)
Achievements and Developments at LLL (*February 1977*)

NATIONAL SECURITY

The Livermore Pool-Type Reactor (*June 1977*)
Imaging Implosion Dynamics: The X-Ray Pinhole/Streak Camera (*December 1976*)

NUCLEAR ENERGY

Western States Uranium Resource Survey (*May 1977*)

PHYSICAL SCIENCES AND ENGINEERING

Probing Nuclei with LLL's Electron Linear Accelerator (*July 1977*)
Mapping Underground Structure with Radio Waves (*January 1977*)
DISPLAY: An Interactive Picture Editor (*January 1977*)

SOLAR, GEOTHERMAL, AND ADVANCED ENERGY SYSTEMS

Laser Fusion Program Overview (*August 1977*)
Taming Geothermal Brines for Electrical Power (*July 1977*)
TMX: A New Fusion Plasma Experiment (*July 1977*)
Wind-Energy Assessment (*June 1977*)

Printed in the United States of America
Available from
National Technical Information Service
U.S. Department of Commerce
5285 Port Royal Road
Springfield, Virginia 22161
Price: Printed Copy $4.00; Microfiche $3.00

PAST TITLES

Articles in the *Energy and Technology Review* have been organized into subject areas approximately corresponding to the Assistant Administrators' areas of responsibility in the Energy Research and Development Administration. These subject areas are listed below with references to some recent articles in each category. (A semiannual index appears in the June and December issues.)

CONSERVATION

Car for Tomorrow: A Quasi-Electric-Drive Vehicle (*June 1977*)
Transportation's Role in the Energy Problem (*March 1977*)
The Methanol Engine: A Transportation Strategy for the Post-Petroleum Era (*December 1976*)

ENVIRONMENT AND SAFETY

Diagnosing Cervical Cancer with Flow Cytometry (*July 1977*)
Phantom Construction: Building a Torso Manikin for Whole-Body Counting (*December 1976*)
Getting the Facts About Ozone (*November 1976*)

FOSSIL ENERGY

Progress in Oil-Shale Research (*February 1977*)
Hoe Creek No. 1: An *In Situ* Coal Gasification Experiment (*January 1977*)

LABORATORY TRENDS

Continuing Education at LLL (*May 1977*)
The Laboratory: Retrospect and Prospect (*February 1977*)
Achievements and Developments at LLL (*February 1977*)

NATIONAL SECURITY

The Livermore Pool-Type Reactor (*June 1977*)
Imaging Implosion Dynamics: The X-Ray Pinhole/Streak Camera (*December 1976*)

NUCLEAR ENERGY

Western States Uranium Resource Survey (*May 1977*)

PHYSICAL SCIENCES AND ENGINEERING

Probing Nuclei with LLL's Electron Linear Accelerator (*July 1977*)
Mapping Underground Structure with Radio Waves (*January 1977*)
DISPLAY: An Interactive Picture Editor (*January 1977*)

SOLAR, GEOTHERMAL, AND ADVANCED ENERGY SYSTEMS

Laser Fusion Program Overview (*August 1977*)
Taming Geothermal Brines for Electrical Power (*July 1977*)
TMX: A New Fusion Plasma Experiment (*July 1977*)
Wind-Energy Assessment (*June 1977*)

Printed in the United States of America
Available from
National Technical Information Service
U.S. Department of Commerce
5285 Port Royal Road
Springfield, Virginia 22161
Price: Printed Copy $4.00; Microfiche $3.00